Aerodynamic characterization of model vegetation by wind tunnel experiments

Author(s):
Manickathan, Lento; Defraeye, Thijs; Allegrini, Jonas; Derome, Dominique; Carmeliet, Jan

Publication date:
2016-05

Permanent link:
https://doi.org/10.3929/ethz-b-000303904

4th International Conference on Countermeasures to Urban Heat Island, 30-31 May and 1 June 2016,
National University of Singapore, Singapore

Aerodynamic characterisation of model vegetation by wind tunnel experiments

Manickathan L[1,2], Defraeye T[1,2], Allegrini J[1,2], Derome D[2] and Carmeliet J[1,2].
[1] Chair of Building Physics, ETH Zürich, Stefano-Franscini-Platz 5, 8093 Zürich, Switzerland
[2] Laboratory for Multiscale Studies in Building Physics, Empa, Überlandstrasse 129, 8600 Dübendorf, Switzerland
Email: manickathan@arch.ethz.ch, defraeye@arch.ethz.ch, jonas.allegrini@empa.ch, dominique.derome@empa.ch, carmeliet@arch.ethz.ch

ABSTRACT

A better prediction of turbulent airflow around porous vegetation is required for urban environment studies as vegetation is being increasingly utilized to mitigate Urban Heat Islands (UHI). Trees in urban areas impact ventilation by disturbing the flow and lead to cooling by evapotranspiration. Furthermore, trees have been shown to play a role in pollutant removal. A first step in properly accounting for the impact of vegetation on UHI is to accurately determine the heat and mass exchange between vegetation and the environment. For such determination, an accurate model of the turbulent flow field around vegetation and an improved parameterisation of the turbulent momentum deficit using drag coefficient must be obtained.

The aim of this paper is to investigate the drag profile and turbulent flow field of flexible and inflexible model trees. The drag coefficients of model trees are measured using a force balance and the turbulent flow fields are measured using a stereo-PIV setup.

This paper provides a mean to better predict the turbulent airflow within and around porous vegetation by studying the relation of drag coefficients with turbulent flow fields for model trees. The drag coefficients of inflexible model trees are found to be nearly independent of wind speed whereas, for the flexible model with leaves and branches that streamline to the flow field, the drag coefficients decrease with increasing wind speed. These finding agree with the literature. The normalized mean velocity is related to the drag coefficient, where velocity deficit increases with the drag. Investigating the mean Reynolds stress component does not yield a definite correlation with drag coefficient.

Key Words: urban heat island, vegetation, model tree, wind tunnel, stereo PIV, drag coefficient

1. INTRODUCTION

Vegetation is being increasingly utilized in urban environments to mitigate the Urban Heat Island (UHI) effect, which frequency and magnitude are increasing due to increasing urbanisation and could be further magnified by climate change. Urban reforestation/revegetation strategies are expected to provide counter-UHI effects, as indicated in a few studies, such as cooling due to evapotranspiration and shading (Alexandri and Jones, 2008; Loughner et al., 2012) and can have an impact on the greenhouse gases such as CO_2 (Nowak et al., 2006). Combination of these effects could result in improved human health and comfort in urban areas.

Assessing the effects of vegetation in urban environments can be quantified using urban microclimate models, as they provide means to understand the governing factors of UHI effect (Amorim et al., 2013; Bruse and Fleer, 1998; Robitu et al., 2006; Saneinejad et al., 2012). However, most current microclimate models use a simplified modelling of momentum exchange of vegetation with the environment by using empirical drag coefficients. The drag coefficient of vegetation is assumed to be constant and independent of wind speed and direction. In literature, vegetation drag coefficients typically can range from 0.1 to 0.3, depending on the species (Wilson and Shaw, 1977). However, to accurately determine the heat and mass exchange between the vegetation and the environment, accurate drag coefficient versus velocity relationships are

required. Additionally, the turbulent momentum exchange between the vegetation and its surrounding needs to be characterized.

In literature, several studies investigate the drag coefficient variations of model and natural trees. Gromke and Ruck (2008) perform an experimental study of inflexible small model trees with spherical crowns. The drag coefficient of inflexible models is found to be independent of velocity. Investigating for a natural, flexible tree, Rudnicki et al. (2004) and Vollsinger et al. (2005) observe the effect of pruning and streamlining on the drag coefficient. For flexible natural trees, the drag coefficient decreases with increasing wind speed. Cao et al. (2012) show drag coefficients increasing with volumetric density for unpruned and pruned natural trees and decreasing at higher wind speeds.

To the authors' knowledge, detailed experimental investigation of the correlation of the turbulent flow field around vegetation and its drag coefficient was not thoroughly studied in literature. In this paper, the time-averaged velocity field and the Reynolds stress component are investigated in addition to measuring the drag coefficient and correlations are examined. The drag coefficient of the trees is measured using a force balance and the flow field around the vegetation using Particle Image Velocimetry (PIV) technique.

2. METHODOLOGY

In this section, the experimental design, the data acquisition and the data calculation method are described. The vegetation models are first described in section 2.1. Section 2.2 describes the overall configuration of the vegetation models in the wind tunnel. The measurement and the calculation of the drag coefficient are elaborated in section 2.3 and finally the PIV technique used for measuring the flow around the vegetation is detailed in section 2.4.

2.1. Vegetation models

Four different model trees are used for the present investigation, as shown in contrast images in Figure 1. To determine the dimensions (height and frontal area) of the model, a reference background is placed behind the models and lens distortion correction is applied.

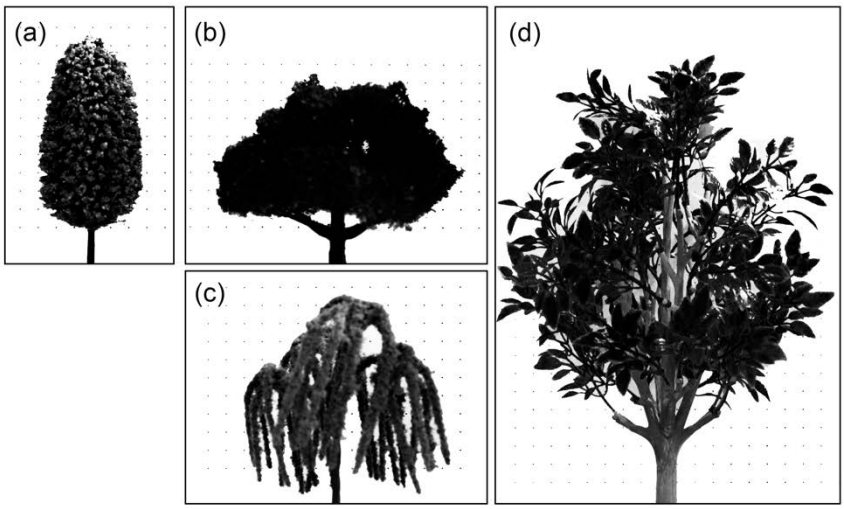

Figure 1: High contrast images of four model trees: (a) model tree 1, (b) model tree 2, (c) model tree 3 and (d) model tree 4. The dots in background are 10mm apart.

Table 1: Model tree specifications.

Model tree ID	Height H (m)	Frontal Area (no wind) A (m^2)	Flexible
1	0.1275	0.0059	yes
2	0.11	0.0086	no
3	0.12	0.0067	yes
4	0.26	0.0226	yes

The specifications of these models are summarised in Table 1. In this study, two types of vegetation are primarily used. Model trees 1, 2, and 3 are small model trees made of polymeric materials with different rigidity, porosity, shape and height. Model tree 4 is a larger model, with individual polymeric thin leaves mimicking those of a natural tree and the branches and trunk are made of flexible polymer. Its branches and leaves streamline at high wind speeds similar to a natural tree. Figure 2 shows the shape of model tree 4 at no wind condition and at 15 m/s, where the deformation due to streamlining is visible.

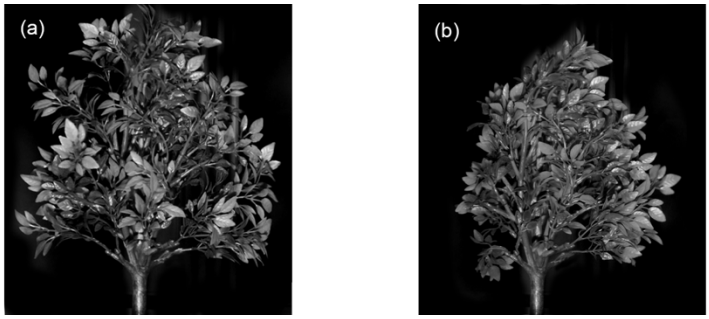

Figure 2: Variation in the shape of model tree 4: (a) at no wind condition and (b) at 15 m/s. At 15 m/s the branches and leaves of the model streamline with the flow field.

2.2. Experimental setup

The wind tunnel experiment is performed in the ETHZ/Empa Atmospheric Boundary Layer (ABL) wind tunnel. It is a closed circuit Göttingen type wind tunnel with a test section cross-section of 1.9 m (width) by 1.3 m (height). The wind tunnel is able to provide wind speeds ranging from 0.5 to 25 m/s.

The test section is modified to expose the model trees to uniform free-stream flow, out of the turbulent boundary layer on the wind tunnel floor (Immer, 2015). This is achieved by installing a split-floor downstream of the test section, as depicted in Figure 3, near uniform velocity profile at the force balance. The model tree is placed on the force balance plate, enabling the measurement of force at various wind speeds. A stereoscopic PIV setup observes a Field of View (FOV) of approximately 400×400 mm above the force balance plate, aiming at measuring the flow field in the symmetry plane.

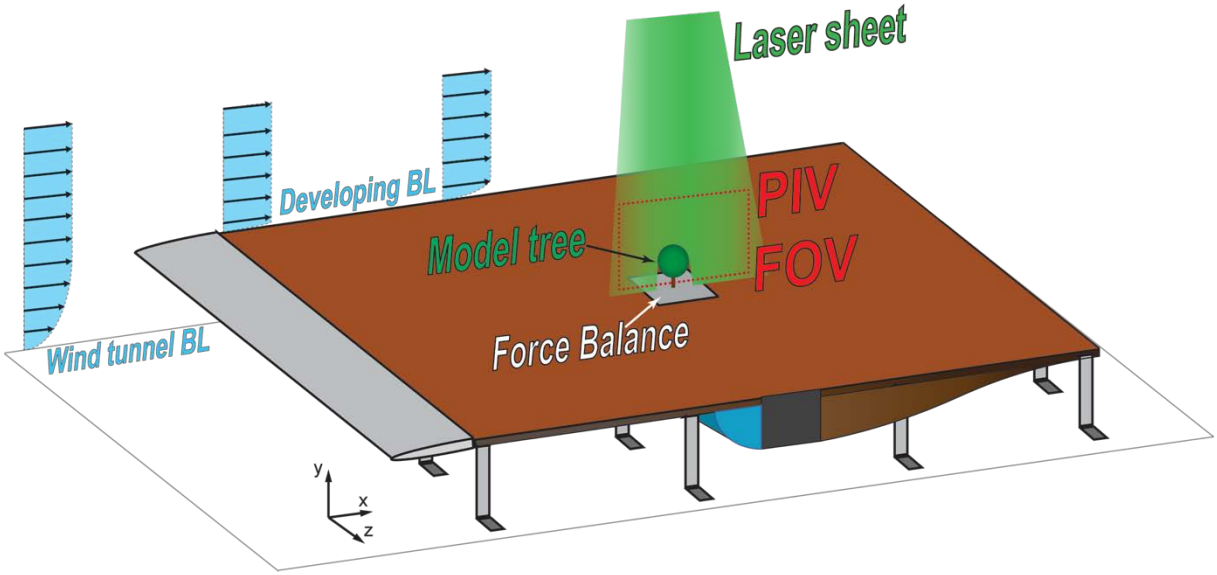

Figure 3: Wind tunnel setup for combined measurement of flow field and force acting on the model using a split floor downstream of the wind tunnel test section. Model tree is placed on the force balance, with a PIV Field of View of approximately 400×400 mm.

2.3. Force measurements

The force acting on the model trees is measured using a 3-axis force balance at an acquisition rate of 2.5 Hz and precision of $\pm$ 0.005 N. The mean force at a given wind speed is determined by time averaging the time series over approximately one minute, obtaining uncorrelated samples with sufficient sample size.

The drag coefficient C_d of tree models measured at various wind speeds is calculated from the following relation (Anderson, 2010):

$$C_d = \frac{2F_D}{\rho U^2 A} \tag{1}$$

where F_D is the drag force in the direction of the wind speed, ρ is the air density, U is the characteristic wind speed and A is the frontal area. The wind speed U is determined directly from the wind tunnel pitot-static tube and the frontal area A of the trees is calculated directly from the high contrast images shown in Figure 1. The drag coefficient versus wind speed curve is generated by sampling from 3 to 20 m/s, at 1 m/s interval. The spread of the drag coefficient is determined using multiple measurements at two different wind directions (0º and 90º orientation).

In this study, the frontal area A of the models is taken to be the static frontal area, i.e. without wind. Another approach is to use the dynamic front area A_{dyn}, where the frontal area is specific to a given wind speed (Rudnicki et al., 2004). However, for this study, we limited our focus to the static drag coefficient, to allow a comparison with literature (Gromke et al. 2008; Rudnicki et al., 2004; Vollsinger et al., 2005). In future work, the authors will use the dynamic frontal area in order to characterize also the dynamic drag coefficient.

2.3. PIV setup

The flow around the vegetation is measured using Particle Image Velocimetry (PIV). PIV is a non-intrusive approach for measuring velocity fields in fluid flow. The principle of a PIV measurement is quantifying the motion of tracer particles in the flow, by correlating two particle images of a known time interval dT. The tracer particles are illumined using a double-cavity Nd-YAG laser producing two collimated light beams at 532 nm (green light). The laser illuminates a 2D (x-y) plane, coinciding with the vertical plane at the centre of the trunk of the model tree, as shown in Figure 3. However, as vegetation has non-symmetric heterogeneously distributed foliage, an out-of-plane velocity component is present in this 2-D plane. Therefore, a stereoscopic PIV (stereo-PIV) setup is used to measure all the components of the velocity. The stereo-PIV employs two sCMOS cameras looking from two angles to determine the out-of-plane velocity component.

A severe limiting factor during the measurements is the strong reflections from the floor and the different surfaces of the vegetation, oversaturating the camera imaging chip and resulting in low signal-to-noise ratio. Oversaturated regions are removed by physically placing a mask between the camera and the objects (floor and model tree). The airflow measurements are performed at three wind speeds (3, 10 and 15 m/s). Time-averaged flow fields are obtained from 1000 snapshots acquired at 15 Hz, to obtain uncorrelated images of sufficient sample size. The time interval dT is modified depending on the wind speed to obtain a 1/4th pixel shift in a 32-by-32 cross-correlation interrogation window (at 50% overlap). The data is acquired and processed using Dantec Dynamics PIV system.

4. RESULTS AND DISCUSSION

4.1. Drag coefficient

The drag coefficient C_d of the model trees is determined by using Equation (1). Figure 4a shows the drag coefficient C_d as a function of Reynolds number Re:

$$Re = \frac{\rho U L}{\mu} \tag{2}$$

where the characteristic length L is taken to be the height H of the models. Investigation the relationship of the drag coefficient C_d with Reynolds number Re provides a better means of comparison for different vegetation types. The figure shows mean values (solid lines) and the spread (solid area) obtained from multiple measurements at two different wind directions. The drag coefficients of model tree 1, 2, and 3 are decreasing slightly with increasing Reynolds number, and averaged at about 0.6, 0.7, and 0.8, respectively. The drag coefficient of model tree 4 initially increases slightly, peaking at approximately 0.85 at $Re = 1 \times 10^5$ and decreases substantially towards $C_d = 0.7$ at higher Reynolds number. Furthermore, in comparison to the other models, the range of the Reynolds number for model tree 4 is shifted to a higher value due to its larger height of $H = 0.26$.

Model tree 3 exhibits a large spread on the drag coefficient due to its unusual, non-axisymmetric geometry and flexibility, unlike other model trees. Model trees 1, 2 and 4 undergo less deformation resulting in a smaller spread in the drag coefficient with wind direction.

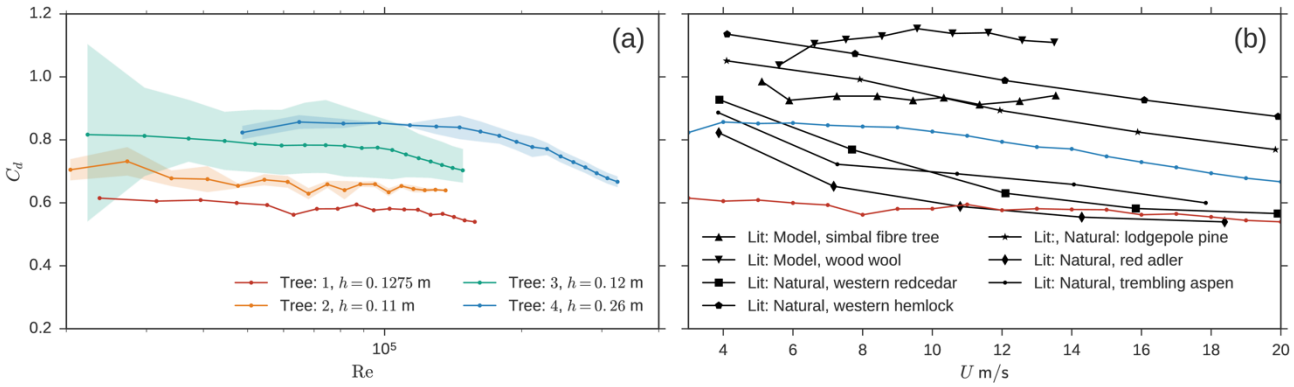

Figure 4: Drag Coefficient C_d of (a) model trees as function of Reynolds number Re and (b) as function of wind speed U, including data from literature for model trees (Gromke and Ruck, 2008) and natural trees (Rudnicki et al., 2004; Vollsinger et al., 2005).

A comparison of the results for model trees 1 and 4 with literature is performed in Figure 4b. The drag coefficient of trees is plotted as a function of wind speed, as Reynolds numbers were not available from the literature sources. As mentioned above, the study of Gromke and Ruck (2008) provides drag coefficient of small inflexible model trees while the studies of Rudnicki et al. (2004) and Vollsinger et al. (2005) provide the characteristics of natural trees. The figure shows that the drag measurement of the present study agrees reasonably well with literature. Model tree 1 exhibits a near-constant drag coefficient, similar to the study of Gromke and Ruck (2008) for inflexible model trees.

The present study shows that, for tree models that do not streamline to the flow field (model trees 1, 2, and 3), the drag coefficient is almost independent of the wind speed. This could simplify the experimental characterisation of the drag coefficient as only one C_d would need to be measured. However, for tree models that display behaviour similar to natural trees (model tree 4), the drag coefficient shows a non-linear behaviour and decreases as higher wind speed. Similar characteristics are observed for natural trees (Rudnicki et al., 2004; Vollsinger et al., 2005). However, the impact of variance on the flexibility of the natural trees needs to further investigated and characterized. Furthermore, the underlying issue with scaling of the trees needs to further investigated because the mechanical property of the natural trees is different to the small models.

4.2 Flow field around vegetation

The understanding of the interaction of vegetation with the airflow is further expanded by investigating the flow field. Figure 5 shows the normalized time-averaged velocity norm $\overline{\boldsymbol{u}}/U_\infty$, overlapped with flow streamlines. The figure axis is normalized by the height of model tree 4

(right), where $H = 0.26\,m$. In the vicinity of the vegetation and the floor, the flow cannot be measured due to masking of zones with high reflections.

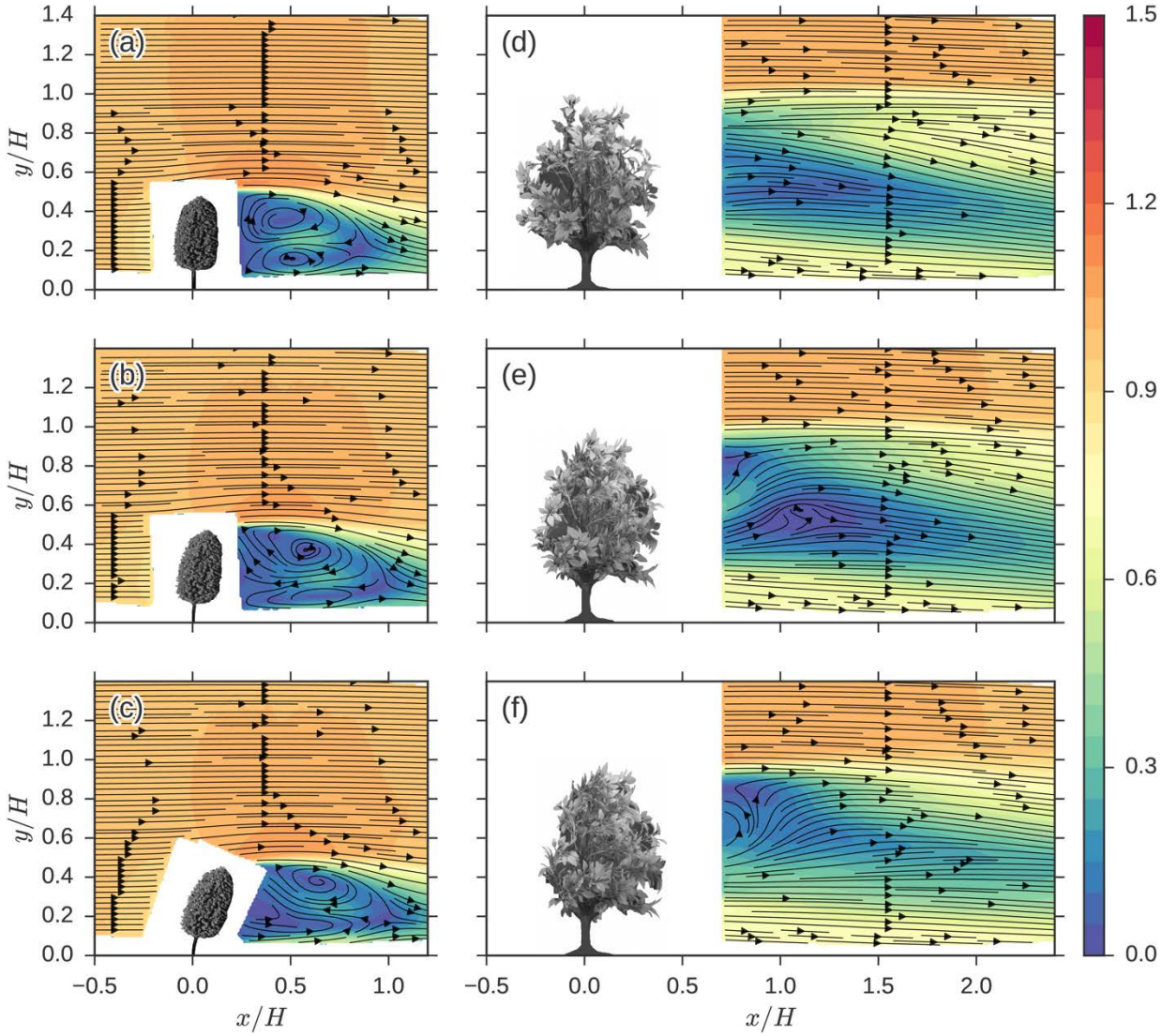

Figure 5: Normalized mean (time-averaged) velocity norm $|\bar{\boldsymbol{u}}|/U_\infty$ of model tree 1 (a, b and c) and model tree 4 (d, e and f). PIV measurements are performed at freestream velocity U_∞ of 3 m/s (a and e), 10 m/s (b and e) and 15 m/s (c and f).

Downstream of the vegetation, a velocity deficit can be observed in all cases indicating the wake of the vegetation. For model tree 1, the wake is more prominent, with distinct recirculation zones extending in a length equal to twice the vegetation height. The shape of the recirculation also varies slightly due to the bending of the model. Comparing the flow fields of tree 1 with those of tree 4, we see that tree 4 does not have a distinguishable recirculation zone. Instead, bleed flow appears through the tree due to its higher porosity, leading to a higher mass flow through the vegetation.

Investigating the strength of the wake behind tree 4, we observed that, at 10 m/s, the vegetation exhibits the greatest velocity deficit, followed by 3 m/s and finally 15 m/s. The trend in velocity deficit thus correlates with the trend of drag coefficient of the model, where a peak in drag coefficient is observed at medium wind speeds. As such, the drag force measurements could be used to identify the interesting speeds at which the flow fields will differ from others, for subsequent PIV measurements.

A further understanding of the turbulent momentum exchange of the vegetation and the flow is determined by investigation the Reynolds stresses. Figure 6 shows the normalized mean Reynolds stress component $R_{12}^* = \overline{u'v'}/U_\infty^2$. The figure shows that the normalized component R_{12}^* increases slightly with wind speed. The effect is most prominent for tree 4, Figure 6(d, e and f). However, the

figure also shows that there is no noticeable correlation between the drag coefficient and Reynolds stress component R_{12}^*, as no peak magnitude is observed in medium wind speeds, Figure 6e. Furthermore, the Reynolds stress component appears to be largest in regions of high velocity gradients such as at the canopy of the vegetation and the base of the foliage. Similar investigation can be performed with the other Reynolds stress components and provides an interesting topic for future research.

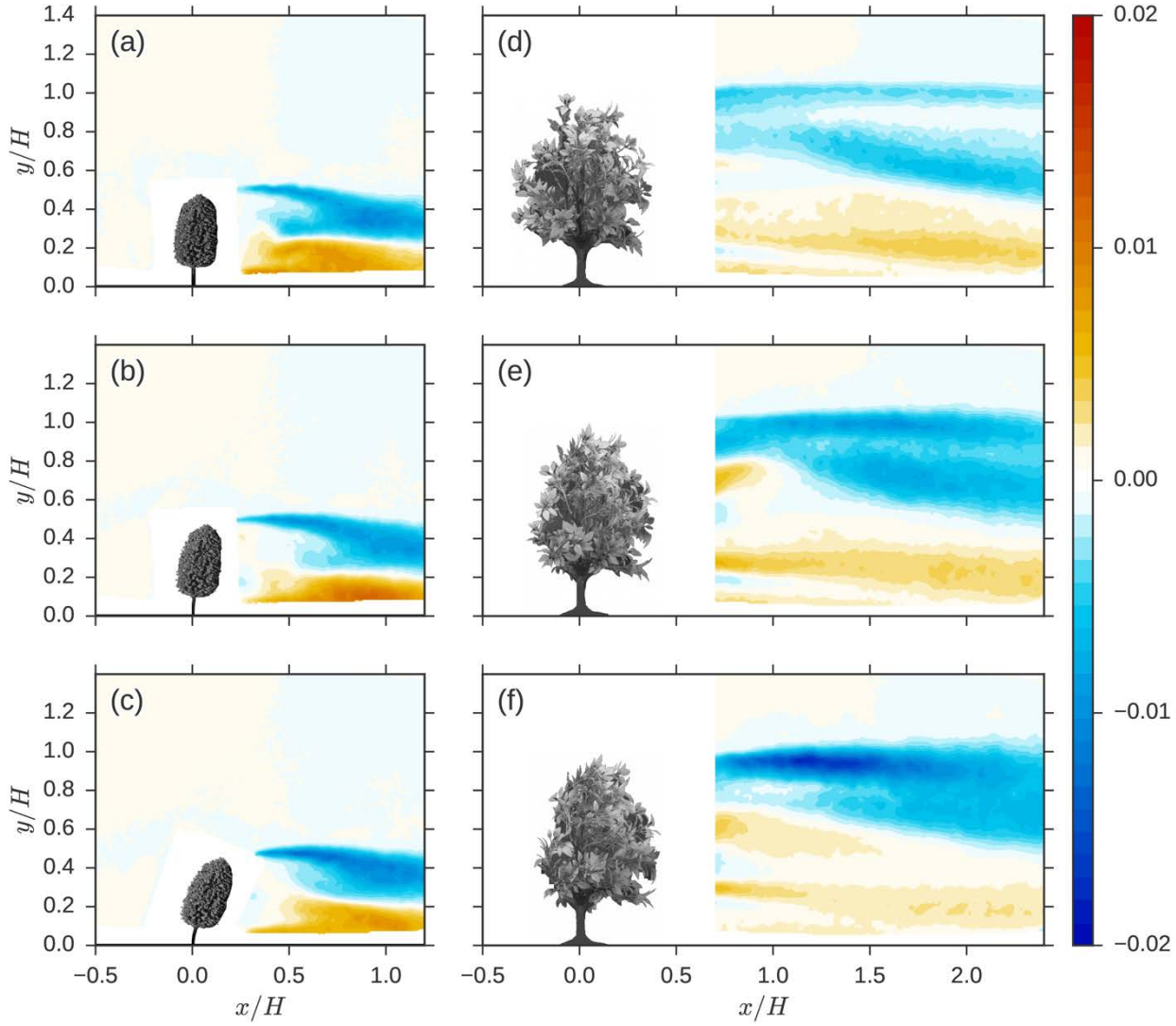

Figure 6: Normalized mean Reynolds shear-stress $R_{12}^* = \overline{u'v'}/U_\infty^2$ of model tree 1 (a, b and c) and model tree 4 (d, e and f). PIV measurements are performed at freestream velocity U_∞ of 3 m/s (a and e), 10 m/s (b and e) and 15 m/s (c and f).

5. CONCLUSION

The aerodynamic characterisation of vegetation models is performed using wind tunnel measurements, involving the measurement of drag coefficients and turbulent flow fields for flexible and inflexible tree models. This study measures the drag coefficient of four model trees from velocities ranging from 3 to 20 m/s, using a force balance. The measurements agree well with the literature data for inflexible model trees and flexible natural trees. The drag coefficient of inflexible models is nearly independent of the wind speed, where as the one of the flexible model decreases with increasing wind speed. This is attributed to the streamlining of the foliage to the flow field.

Subsequently, the correlation of the turbulent flow field of the model trees with drag coefficient is investigation using Particle Image Velocimetry (PIV). The normalized mean velocity norm $|\overline{\boldsymbol{u}}|/U_\infty$ reflects the trend of drag coefficient where velocity deficit in the wake decreased with decreasing drag coefficient. By investigating the normalized mean Reynolds stress component

$\overline{u'v'}/U_\infty^2$, a distinct correlation with the drag coefficient is not observable, but this stress component is observed to be largest in regions of high velocity gradient such as at the edge of canopy and base of the foliage.

In future works, the present results will be used to validate CFD simulations in order to explore the impact of vegetation in urban microclimate. Furthermore, the present experimental study will be expanded to turbulent flow field around natural trees and turbulent flow field within the vegetation using a Refractive-Index-Matching (RIM) water tunnel.

ACKNOWLEDGEMENTS

The authors acknowledge the support of Beat Margelisch, Roger Vonbank and Stefan Carl at Empa.

REFERENCES

Alexandri, E., & Jones, P. (2008). Temperature decreases in an urban canyon due to green walls and green roofs in diverse climates. *Building and Environment*, *43*(4), 480–493. http://doi.org/10.1016/j.buildenv.2006.10.055

Amorim, J. H., Rodrigues, V., Tavares, R., Valente, J., & Borrego, C. (2013). CFD modelling of the aerodynamic effect of trees on urban air pollution dispersion. *Science of The Total Environment*, *461-462*, 541–551. http://doi.org/10.1016/j.scitotenv.2013.05.031

Anderson, J. (2010). *Fundamentals of Aerodynamics, 5th Edition*. McGraw-Hill Education.

Bruse, M., & Fleer, H. (1998). Simulating surface–plant–air interactions inside urban environments with a three dimensional numerical model. *Environmental Modelling & Software*, *13*(3-4), 373–384. http://doi.org/10.1016/S1364-8152(98)00042-5

Cao, J., Tamura, Y., & Yoshida, A. (2012). Wind tunnel study on aerodynamic characteristics of shrubby specimens of three tree species. *Urban Forestry & Urban Greening*, *11*(4), 465–476. http://doi.org/10.1016/j.ufug.2012.05.003

Gromke, C., Buccolieri, R., Di Sabatino, S., & Ruck, B. (2008). Dispersion study in a street canyon with tree planting by means of wind tunnel and numerical investigations - Evaluation of CFD data with experimental data. *Atmospheric Environment*, *42*(37), 8640–8650. http://doi.org/10.1016/j.atmosenv.2008.08.019

Gromke, C., & Ruck, B. (2008). Aerodynamic modelling of trees for small-scale wind tunnel studies. *Forestry*, *81*(3), 243–258. http://doi.org/10.1093/forestry/cpn027

Immer, M. (2015). *Time-resolved measurement and simulation of local scale turbulent urban flow*. ETH Zürich.

Loughner, C. P., Allen, D. J., Zhang, D.-L., Pickering, K. E., Dickerson, R. R., & Landry, L. (2012). Roles of Urban Tree Canopy and Buildings in Urban Heat Island Effects: Parameterization and Preliminary Results. *Journal of Applied Meteorology and Climatology*, *51*(10), 1775–1793. http://doi.org/10.1175/JAMC-D-11-0228.1

Nowak, D. J., Crane, D. E., & Stevens, J. C. (2006). Air pollution removal by urban trees and shrubs in the United States. *Urban Forestry & Urban Greening*, *4*(3-4), 115–123. http://doi.org/10.1016/j.ufug.2006.01.007

Robitu, M., Musy, M., Inard, C., & Groleau, D. (2006). Modeling the influence of vegetation and water pond on urban microclimate. *Solar Energy*, *80*(4), 435–447. http://doi.org/10.1016/j.solener.2005.06.015

Rudnicki, M., Mitchell, S. J., & Novak, M. D. (2004). Wind tunnel measurements of crown streamlining and drag relationships for three conifer species. *Canadian Journal of Forest Research*, *34*(3), 666–676. http://doi.org/10.1139/x03-233

Saneinejad, S., Moonen, P., Defraeye, T., Derome, D., & Carmeliet, J. (2012). Coupled CFD, radiation and porous media transport model for evaluating evaporative cooling in an urban environment. *Journal of Wind Engineering and Industrial Aerodynamics*, *104-106*, 455–463. http://doi.org/10.1016/j.jweia.2012.02.006

Vollsinger, S., Mitchell, S. J., Byrne, K. E., Novak, M. D., & Rudnicki, M. (2005). Wind tunnel measurements of crown streamlining and drag relationships for several hardwood species. *Canadian Journal of Forest Research*, *35*(5), 1238–1249. http://doi.org/10.1139/x05-051

Wilson, N. R., & Shaw, R. H. (1977). A Higher Order Closure Model for Canopy Flow. *Journal of Applied Meteorology*, *16*(11), 1197–1205. http://doi.org/10.1175/1520-0450(1977)016<1197:AHOCMF>2.0.CO;2